# High-Frequency LC$^3$L Resonant DC-DC Converter for Automotive LED Driver Applications

Satyaki Mukherjee*, Alihossein Sepahvand†, Dragan Maksimović†

*Indian Institute of Technology, Kharagpur
Email: {satyaki.mukherjee}@ee.iitkgp.ernet.in

†Colorado Power Electronics Center
Department of Electrical, Computer and Energy Engineering
University of Colorado, Boulder, CO 80309-425, USA
Email: {ali.sep, maksimov}@colorado.edu

***Abstract*—This paper presents a high-frequency zero-voltage switching (ZVS) resonant converter using a novel LC$^3$L resonant tank. The converter behaves like a current source, with its dc output current independent of the output voltage. This property is favorable for LED driver applications, including automotive lighting. Furthermore, the converter exhibits minimal circulating current over its output voltage range. To reduce radio frequency interference, the converter is designed to operate at switching frequency above the AM frequency band. Experimental results are given for a 2 MHz LC$^3$L converter prototype operating over an output voltage range of 3 V to 50 V while supplying a constant 0.5 A output current to a string of 1-to-15 LEDs. Using Silicon MOSFETs, the prototype achieves a peak efficiency of 89.5%, and maintains greater than 85% efficiency across a wide output voltage range.**

## I. Introduction

In automotive lighting applications, light-emitting diodes (LEDs) with dc-dc drivers are increasingly replacing conventional incandescent lamps [1]–[11]. Advantages of LED based automotive lighting include reduced power consumption, longer lifetime, improved functionality, flexibility, and shorter turn-on time, which is considered important for brake lights [5], [12]. A dc-dc driver is required to efficiently deliver well regulated, low-ripple current to a string of series-connected LED's, as shown in Fig. 1, and must be designed to operate over wide ranges of output and input voltages. Meeting EMI requirements in automotive applications is also challenging. Conventional LED driver dc-dc converters, which typically operate at hundreds of kHz [1], [3], [7]–[10], raise issues with AM radio interference. Fast converter turn on and turn off transitions are required to achieve high resolution dimming using pulse-width modulation of the output current at the rate of 200 Hz to 1 kHz, to avoid flicker. To meet fast turn-on and turn-off times, it is advantageous to minimize the need for large internal energy storage. Depending on the specific lighting application, $N$ is typically between 1 and 15, so that the converter output voltage can be between about 3 V and about 50 V. The converter input is tied to the vehicle low-voltage bus, which is nominally $12-14$ V, but can be as low as $4.5$ V (during cold-start events) or as high as $45$ V (during "load dump" events).

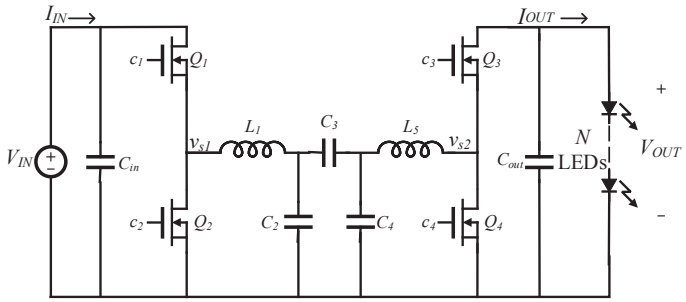


Figure 1: LC$^3$L resonant dc-dc converter for automotive LED driver applications

Standard automotive LED drivers are based on PWM dc-dc converters with buck-boost characteristic, such as a boost converter followed by a buck converter, or a four-switch noninverting buck-boost converter. As a trade-off between size and losses, conventional LED drivers typically operate at hundreds of kilohertz [1], [3], [7]. It is desired to select the switching frequency above the AM frequency band to reduce radio frequency interference, improve power density, and speed up on/off transients in order to improve PWM dimming performance. An approach based on integrated magnetics Ćuk converter has been described in [13], [14].

Alternatively, soft-switching resonant converters are considered as candidates for further improvements in power density and dynamic performance. They open opportunities to overcome limitations of conventional approaches, and are potentially viable candidates for high performance automotive LED driver applications. For example, LED drivers based on the LLC resonant tank [15] have been considered in [16].

978-1-5386-1180-7/18/$31.00 ©2018 IEEE

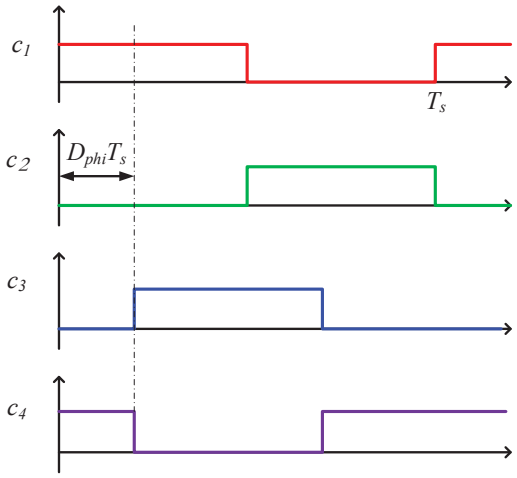


Figure 2: Switch control signals. The converter is controlled by phase shift $D_{phi}$ between the inverter and the rectifier half-bridge

However, higher circulating current at light load results in reduced efficiency, making the LLC resonant dc-dc converter less well-suited for an automotive LED driver application with wide input and output voltage ranges.

This paper introduces an LC$^3$L resonant dc-dc converter for automotive LED driver applications, illustrated in Fig. 1. The proposed LC$^3$L resonant dc-dc converter, when appropriately designed, produces a constant current to a string of LEDs and maintains ZVS operation with minimal circulating current across a wide output voltage ranges. As loading decreases, the proposed converter's input impedance increases, which minimizes circulating current. To achieve soft switching, the converter switching frequency is selected such that the resonant tank input impedance is slightly inductive. This results in a slight deviation from the ideal constant current source operation of the converter. Hence, a control strategy is proposed to tightly regulate the output current while maintaining soft switching.

The paper is organized as follows. Section II presents operation and analysis of the proposed LC$^3$L resonant dc-dc converter shown in Fig. 1. The resonant tank design is described in Section III. Control objective and modeling of the converter are discussed in Section IV. Experimental and simulation results are presented in Section V. Section VI concludes the paper.

## II. LC$^3$L DC-DC Resonant Converter Current Source Property

The converter schematic is shown in Fig. 1 and the switch control signals are illustrated in Fig. 2. A half-bridge inverter, consist of $Q_1$ and $Q_2$, supplies a resonant network, consist of $L_1$, $L_2$, $C_2$, $C_3$ and $C_4$, with a high-frequency pulsating voltage. The resonant network may provide a voltage step-up or step-down. The second half-bridge, consist of $Q_3$ and $Q_4$, then rectifies the ac output of the resonant network into the converter's dc output voltage. The control signal $c_1$ and $c_2$ are complimentary, with deadtime, to driver the inverter stage. Similarly, control signal $c_3$ and $c_4$ are used to driver the rectifier stage. Control signals $c_1$ and $c_3$ are phase shifted by $D_{phi}T_s$ to achieve ZVS.

Sinusoidal approximation, considering only the first harmonic of the waveforms [17], is utilized to analyze the resonant tank based on the equivalent circuit model shown in Fig. 3. The inverter stage is modeled as a sinusoidal voltage source with amplitude $V_M = \frac{2V_{IN}}{\pi}$ and the rectifier is modeled with an effective load resistance $R_r = \frac{2V_{OUT}}{\pi^2 I_{OUT}}$.

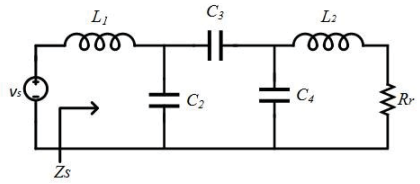


Figure 3: Equivalent circuit model of the resonant tank under sinusoidal approximation.

The tank input impedance seen from the inverter side $Z_s(j\omega)$ is given by:

$$\begin{aligned} Z_s(j\omega) &= X + jY \\ &= j\omega L_1 + \frac{1}{\omega C_2} || (\frac{1}{\omega C_3} + (\frac{1}{\omega C_4}) || (\omega L_2 + R_r)) \end{aligned} \tag{1}$$

where

$$R_r = \frac{2V_{OUT}}{\pi^2 I_{OUT}} \tag{2}$$

assuming that $Q_3$ and $Q_4$ act as an ideal synchronous rectifier. To ensure minimum circulating current in the tank, it is desired to design the resonant tank such that the imaginary part $Y$ in Eqn. (1) is zero. A design that ensures this is given by:

$$C_2 = \frac{2(L_1 - 2L_2)}{L_1(L_1 - 4L_2)\omega^2} \tag{3}$$

$$C_3 = C_4 = \frac{2}{(4L_2 - L_1)\omega^2} \tag{4}$$

It is interesting to note that these design equations have no dependence on the converter's output voltage or power, hence ensuring that circulating currents are minimized regardless of the output voltage, i.e., regardless of the number of series-connected LEDs. Under the design constraints given by Eqn. (3) and Eqn. (4), the resistive tank input impedance is given by:

$$Z_s = X = \frac{\omega^2 L_1^2}{4R_r} \tag{5}$$

The dc input current is given by:

$$I_{IN} = \frac{2V_{IN}}{\pi^2 \frac{\omega^2 L_1^2}{4R_r}} = \frac{16 V_{IN} V_{OUT}}{\pi^4 \omega^2 L_1^2 I_{OUT}} \tag{6}$$

Eqn. (6) indicates that for a constant output current $I_{OUT}$, as the number of LEDs decreases, the magnitude of the tank input current also decreases. Assuming lossless conversion

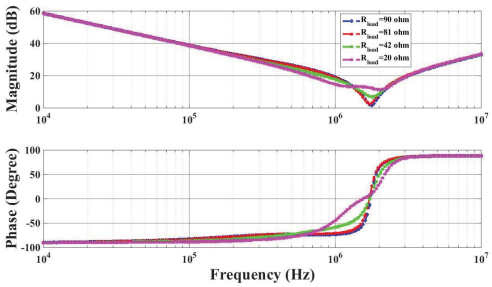


Figure 4: Magnitude and phase plot of the tank input impedance at different loading conditions

($V_{IN}I_{IN} = V_{OUT}I_{OUT}$), a design equation for $L_1$ can be found from

$$I_{OUT} = \frac{4V_{IN}}{\pi^2 L_1 \omega} \tag{7}$$

## III. Prototype Design

From Eqn. (7) it follows that the converter dc output current does not depend on the output voltage and hence on the number of LEDs. Therefore, the converter behaves like a current source, and is capable of supplying a constant current to a string of $N$ LEDs, where $N$ can be variable at design time or during run time. For a given output current, Eqn. (7) can be used to select inductance $L_1$. Then, Eqn. (3) yields the tank capacitances. However, it should be noted that ideal ZVS and near-ZCS operation requires a slightly inductive input impedance of the resonant tank. To accomplish this, a phase shift between the inverter and rectifier half bridge is adjusted slightly away from the phase shift that results in ideal synchronous rectification and purely resistive input impedance. This makes the input current waveform lagging, which increases circulating current to a level necessary to ensure ZVS, and at the same time decreases the output DC current from the designed value. Hence, a practical design approach is to select the tank components as described above but for a slightly higher output current rating. The approach is illustrated by a 2 MHz prototype design example.

The design specifications and the resulting prototype parameters are summarized in Table I. The driver is to supply $I_{OUT} = 0.5$ A to a string of $N = 1 - 15$ LED's, and the target switching frequency is $f_s = 2$ MHz. The output current selected to design the components is $I_{OUT,design} = 0.75$ A. Then, Eqn. (7) yields $L_1 = 600$ nH for $V_{IN} = 14$ V and $f_s = 2$ MHz. It should be noted that $L_2$ can be chosen somewhat arbitrarily, as long as $2L_2 > L_1$). Choosing $L_2 = 390$ nH, Eqn. (3) is used to select the capacitances $C_2 = 3.95$ nF, and $C_3 = C_4 = 13.2$ nF. The resonant inductor $L_1$ is a custom designed component using RM8 core and 3F45 magnetic material, predicted to dissipate less than 2 W of core and winding losses at the worst-case operating point.

The tanks' input impedance is analyzed using a network analyzer, and the results are shown in Fig. 4. One may observe that the tank input impedance is resistive at $\approx 2$ MHz for a wide variation of load.

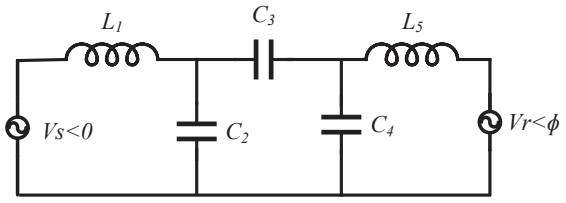


Figure 5: Equivalent circuit model of the resonant tank with applied phase shift

## IV. Converter Modeling and Phase Shift Control

Choosing component values based on an output current somewhat higher than the desired output current specification yields soft switching and regulation of the output current become achievable using the phase shift between the inverter and the rectifier half bridges as the control variable.

### A. Control-to-Output Transfer Function

To design a compensator for closed-loop regulation of the output current, the plant transfer function

$$G_{sys}(s) = \frac{\hat{i}_{OUT}(s)}{\hat{\phi}(s)} \tag{8}$$

is derived first, where $\phi$ is the phase shift between the two half bridges as shown in Fig. 5.

By analyzing the equivalent circuit under sinusoidal approximation, the rms current through the inductor $L_2$ in Fig. 5 is found to be independent of the phase shift and is given by

$$I_{L_2} = \frac{2V_i}{\omega L_1} \tag{9}$$

By operating the rectifier bridge with the phase shift $\phi$, this current is rectified to obtain the output DC current given by

$$I_{out} = \frac{2V_i \cos\phi}{\pi \omega L_1} \tag{10}$$

By linearizing Eqn. (10), the plant transfer function of Eqn. (8) is found as

$$G_{sys}(s) = \frac{\hat{i}_{OUT}(s)}{\hat{\phi}(s)} = \frac{-4V_{IN}\sin\phi}{\pi^2 \omega L_1 (1 + R_{load}C_{out}s)} \tag{11}$$

It should be noted that this expression ignores the resonant tank dynamics. Regulation of the output current can be achieved using a simple closed loop controller with a PI compensator. A high frequency pole is added to attenuate the gain of the compensator at the switching frequency.

### B. Closed-Loop Operation: Simulation Results

To verify the control operation, the transfer function in Eq. (11) is evaluated at a nominal $V_{OUT} = 30$ V ()$N = 9$ LED's) operating point, and a PI compensator is designed to achieve a crossover frequency of 100 kHz. Due to the effect of the high frequency pole, the actual crossover frequency of 77 kHz is obtained, along with a phase margin of $47^o$.

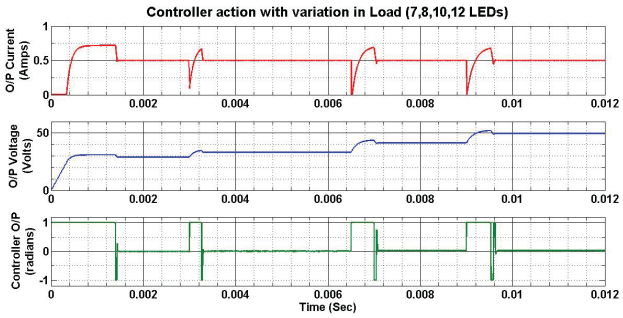


Figure 6: Operation of the closed-loop controlled converter with dynamic changes in the number of LEDs (7-12 LEDs)

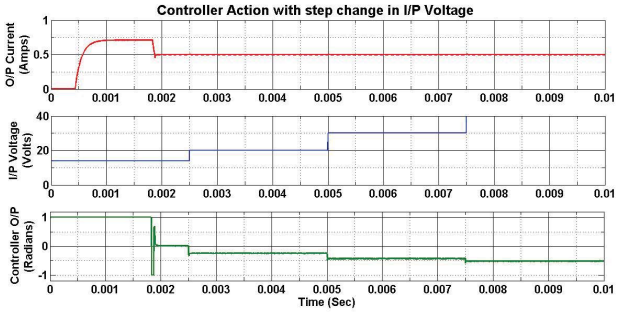


Figure 7: Operation of the closed-loop controlled converter with step changes in the input voltage (10-40 V)

Fig. 6 illustrates operation of the closed-loop controlled converter with dynamic changes in the number of LEDs connected to the output. It can be observed that whenever the number of LEDs increases dynamically, the current initially drops to zero, which causes the controller output to saturate at it's limiting value. As a new LED is inserted in the current path, it has to be forward biased first to allow the output current to build up to the desired reference value. Another important feature is observed during startup, when the current builds up to the maximum possible value of $I_{OUT}$. During start-up, the controller is also saturated, and the converter effectively operates in open loop. Nevertheless, it can be observed that the transients associated with start-up or a dynamic change of the number of LED's are relatively short.

Fig. 7 shows the controller action with variations in input voltage $V_{IN}$. There are no observable changes in the output current as the step changes in $V_{IN}$ occur. The controller operates with the designed bandwidth and regulates the output current at the reference value, except during the start-up transient.

## V. Experimental Results

The 2 MHz prototype was constructed and tested with the components shown in Table I. A photograph of the prototype is shown in Fig. 8. Fig. 9 shows that the output dc current can be regulated to an almost constant value for a given constant phase shift. Also, using $D_\phi$ as a control variable, it is confirmed that very little phase shift variation is sufficient to precisely regulate the output dc current. The change in output current for a particular phase shift across output voltage signifies the boundary of ZVS operation. Below a particular output voltage, the input current is too low to achieve ZVS of the inverter side switches. To regulate the output current across a large variation in output voltage requires very small variations in the phase shift. In other words, very little control effort is required by the controller to achieve output current regulation during normal steady-state operation. Simulation results showing closed-loop responses to large-signal transients have been discussed in Section IV-B.

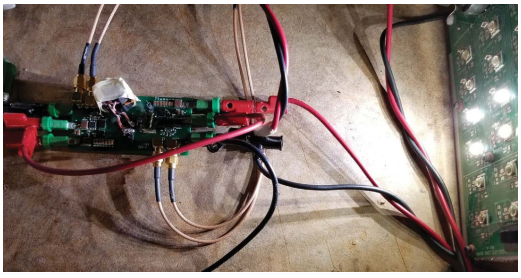

Figure 8: $LC^3L$ resonant dc-dc converter prototype and a test bench with LEDs as the load

Inverter side switch-node voltage $v_{s1}$ and rectifier side switch node voltage $v_{s2}$ along with the switch node currents are shown in Fig. 10 and Fig. 11 for 2 different operating

Table I: Specifications and parameters for the 2 MHz $LC^3L$ prototype converter

| | |
|---|---|
| Switching Frequency $f_s$ | 2 MHz |
| Input Voltage $V_{IN}$ | 14 V nominal, $8-40$ V |
| Output Voltage $V_{OUT}$ | 3 V to 50 V |
| Output Current $I_{OUT}$ | 0.5 A (components designed for 0.75 A) |
| Transistors $Q_1$ to $Q_4$ | Fairchild FDMS86105 |
| Inductor $L_1$ | 600 nH |
| Inductor $L_2$ | 390 nH |
| Capacitor $C_2$ | 3.9 nF |
| Capacitor $C_3$=$C_4$ | 15 nF |
| Gate Drivers | Texas instruments UCC27211 |

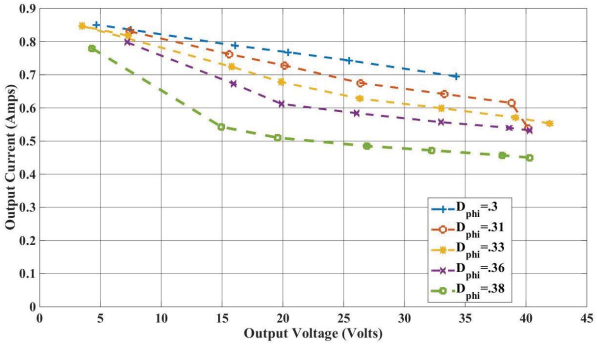


Figure 9: Variation in output current with respect to output voltage at different phase shifts between inverter and rectifier half bridges

points, with input voltage of 14 V, and output voltages of 16 V and 38 V, respectively. Smooth transitions in the switch node voltages indicate ZVS commutation of the transistors at both operating points.

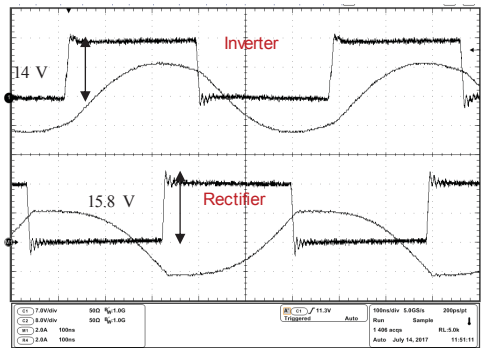


Figure 10: Switch node voltage and current for $N = 5$ LED loading, $V_{IN}$ = 14 V, $V_{OUT}$ = 16 V, $I_{OUT} = 0.5$ A

Fig. 12 and Fig. 13 show the variation in inverter and rectifier side tank current at various loading conditions. One may note that the magnitude of the rectifier side current remains essentially constant over a wide range of operating

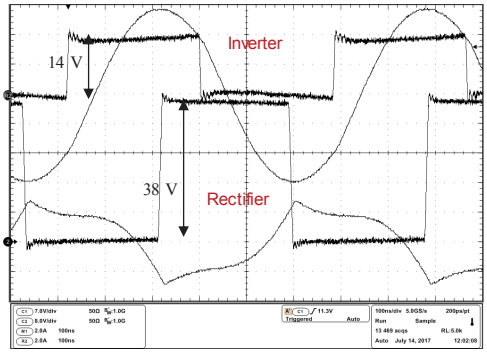


Figure 11: Switch node voltage and current for $N = 12$ LED loading, $V_{IN} = 14$ V, $V_{OUT} = 38$ V, $I_{OUT} = 0.5$ A

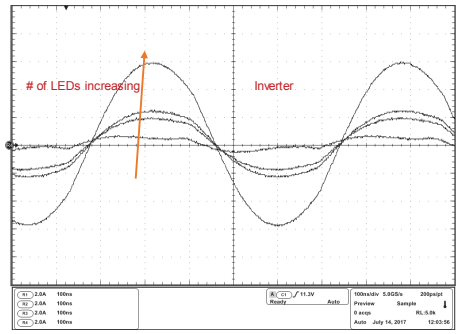


Figure 12: Inverter side current with $V_{OUT}$ varying from 3 V to 38 V, $N = 1 - 12$ (Fig. 1)

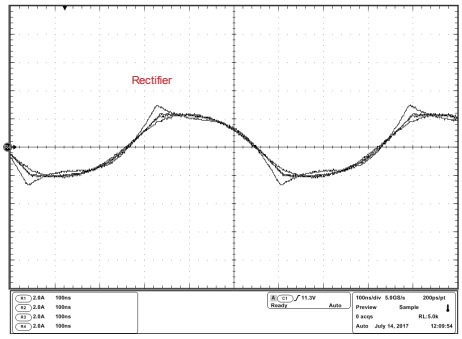


Figure 13: Rectifier side current with $V_{OUT}$ varying from 3 V to 38 V, $N = 1 - 12$ in the converter of Fig. 1

voltage, demonstrating the current source property of the converter. On the other hand, the inverter side current is directly proportional to the loading, which implies that the tank circulating current is minimized.

Experimentally measured efficiency of the prototype for $V_{IN} = 14$ V, $V_{OUT} = 3$ V to 40 V, $I_{OUT} = 0.5$A is plotted in Fig. 14. Greater than 85% power stage efficiency is obtained over a wide range of output voltage (10 V to 40 V). The peak power stage efficiency is 89.5%. These results are comparable to the efficiency performance of state of the art LED drivers [1], [3], [7], [13], [18].

Table II compares the prototype described in this paper to previously reported automotive LED drivers with similar specifications. Advantages of the resonant converter include

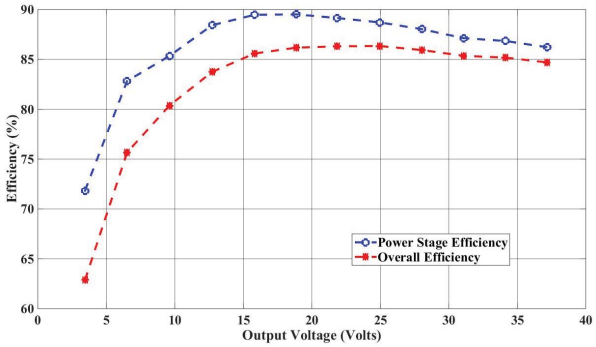


Figure 14: Experimentally measured efficiency for $V_{IN} = 14$ V, $I_{OUT} = 0.5$ A

smaller tank components, and reduced internal energy storage, which implies faster turn on/off capabilities.

Table II: Efficiency and switching comparison for conventional LED drivers and this work.

| Ref. | Peak efficiency | $f_{sw}$(max) | Output power |
|---|---|---|---|
| [1] | 92% | 120 KHz | 30 W |
| [3] | 89.7% | 500 KHz | 40 W |
| [7] | 90% | 350 KHz | 40 W |
| [13] | 85% | 1.8 MHz | 30 W |
| [14] | 93.5% | 2.4 MHz | 30 W |
| **This work** | **89.5**% | **2 MHz** | 30 W |

## VI. Conclusions

A novel LC$^3$L resonant dc-dc converter is described in this paper. The LC$^3$L converter achieves soft-switching and maintains minimal circulating current across wide operating ranges. The converter also features current source output characteristic, making it particularly well suited for automotive LED driver applications. A control technique using phase shift is proposed, to simultaneously regulate the output current, and achieve soft switching of the devices, with minimum control effort. Experimental prototype operates at a switching frequency of 2 MHz (above AM band) over an output voltage range of 3 V to 50 V while supplying a constant 0.5 A output current to a string of 1-to-15 LEDs. Using Silicon MOSFETs, the prototype achieves a peak efficiency of 89.5%, and maintains greater than 85% efficiency across a wide output voltage range.

## Acknowledgment

The work of Satyaki Mukherjee, a visiting scholar with the Colorado Power Electronics Center, was supported in part by S.N. Bose Scholarship.

## References

[1] Y. Wang, S. Gao, Y. Guan, J. Huang, D. G. Xu, and W. Wang, "A Single-stage LED Driver Based on Double LLC Resonant Tanks for Automobile Headlight with Digital Control," *IEEE Trans. Transportation Electrification*, vol. PP, no. 99, pp. 1–1, 2016.

[2] A. Pollock, H. Pollock, and C. Pollock, "High Efficiency LED Power Supply," *IEEE Journal of Emerging and Selected Topics in Power Electronics*, vol. 3, no. 3, pp. 617–623, Sep. 2015.

[3] L. Corradini and G. Spiazzi, "A High-Frequency Digitally Controlled LED Driver for Automotive Applications With Fast Dimming Capabilities," *IEEE Trans. Power Electron.*, vol. 29, no. 12, pp. 6648–6659, Dec. 2014.

[4] X. Qu, S. C. Wong, and C. K. Tse, "A current balancing scheme with high luminous efficacy for high-power led lighting," *IEEE Transactions on Power Electronics*, vol. 29, no. 6, pp. 2649–2654, June 2014.

[5] S. Saponara, G. Pasetti, N. Costantino, F. Tinfena, P. D'Abramo, and L. Fanucci, "A Flexible LED Driver for Automotive Lighting Applications: IC Design and Experimental Characterization," *IEEE Trans. Power Electron.*, vol. 27, no. 3, pp. 1071–1075, Mar. 2012.

[6] L. Ying-yan, Z. Jing, Z. Xue-cheng, and L. Wei, "An Efficiency-enhanced Low Dropout Linear HB LED driver for Automotive Application," in *Proc. IEEE Int. Conf. Electron. Devices and Solid-State Circuits*, 2008, pp. 1–4.

[7] Linear Technologies. (2016) *LT3761A Technical Datasheet*. [Online]. Available: https://cds.linear.com/docs/en/datasheet/3761af.pdf

[8] Texas Instruments. (2016) TLC59116-Q1 16-Channel FM+$I^2$ Constant-Current LED Sink Driver. [Online]. Available: http://www.ti.com/lit/ds/symlink/tlc59116-q1.pdf

[9] Supertex Inc. (2008) *AT9933 Technical Datasheet*. [Online]. Available: http://ww1.microchip.com/downloads/en/DeviceDoc/at9932.pdf

[10] ON Semiconductor. (2012) *1.0A Constant Current Buck Regulator for Driving High Power LEDs*. [Online]. Available: http://www.onsemi.com/pub_link/Collateral/NCL30160-D.PDF

[11] P. Giannelli, L. Capineri, G. Calabrese, G. Frattini, and M. Granato, "A reduced output ripple step-up dc-dc converter for automotive led lighting," in *2017 13th Conference on Ph.D. Research in Microelectronics and Electronics (PRIME)*, June 2017, pp. 329–332.

[12] D. Gacio, J. Cardesin, E. Corominas, J. Alonso, M. Dalla-Costa, and A. Calleja, "Comparison Among Power LEDs for Automotive Lighting Applications," in *Proc. IEEE Ind. Applicat. Soc. Annu. Meeting, (IAS)*, 2008, pp. 1–5.

[13] A. Sepahvand, M. Doshi, V. Yousefzadeh, J. Patterson, K. Afridi, and D. Maksimovic, "Automotive LED Driver Based on High Frequency Zero Voltage Switching Integrated Magnetics Cuk converter," in *Proc. IEEE Energy Convers. Congr. Expo.*, 2016, pp. –.

[14] A. Sepahvand, M. Doshi, V. Yousefzadeh, J. Patterson, K. K. Afridi, and D. Maksimovic, "High-frequency zvs uk converter for automotive led driver applications using planar integrated magnetics," in *2017 IEEE Applied Power Electronics Conference and Exposition (APEC)*, March 2017, pp. 2467–2474.

[15] B. Yang, F. C. Lee, A. J. Zhang, and G. Huang, "Llc resonant converter for front end dc/dc conversion," in *APEC. Seventeenth Annual IEEE Applied Power Electronics Conference and Exposition (Cat. No.02CH37335)*, vol. 2, 2002, pp. 1108–1112 vol.2.

[16] S. D. Simone, C. Adragna, C. Spini, and G. Gattavari, "Design-oriented steady-state analysis of llc resonant converters based on fha," in *International Symposium on Power Electronics, Electrical Drives, Automation and Motion, 2006. SPEEDAM 2006.*, May 2006, pp. 200–207.

[17] R. Erickson and D. Maksimovic, *Fundamentals of Power Electronics*. Springer, 2001.

[18] W. Lin, X. Yuzhen, and Q. L. Zheng, "A high efficiency integrated step-down cuk and flyback converter for led power driver," in *2015 9th International Conference on Power Electronics and ECCE Asia (ICPE-ECCE Asia)*, June 2015, pp. 60–64.